Assimilation Control of a Robotic Exoskeleton for Physical Human-Robot Interaction

Guoxin Li, Zhijun Li, *Fellow, IEEE*, and Zhen Kan, *Member, IEEE*

***Abstract*—The ability of human operators in estimating the partners' motion intention and utilizing it for collaboration brings valuable enlightenment to human-robot systems. Motivated by these observations, this letter introduces an assimilation control method that reshapes the physical interaction trajectory in the interaction task, which enables the exoskeleton robot to estimate the subject's virtual target from the interaction force and adapt its own behavior. Under the assumption that the virtual target is determined by the control gains, the stability of the human-robot system is guaranteed, and the proposed scheme realizes continuous interaction behaviors from cooperation to competition. Then an adaptive controller is designed to enable the robot to directly deal with uncertain dynamics and joint space constraints. The experiment verifies how the assimilation control method assists the subjects in a collaborative execution or gradually competes with them to avoid collisions. Compared with related literature, our approach is able to realize safe manipulation (e.g., obstacle avoidance) and broader interaction behaviors by reshaping the interactive trajectory using force feedback only, without continuous manual guidance as in many existing methods.**

***Index Terms*—Physical human-robot interaction, intention recognition, assimilation control, safety in HRI.**

I. Introduction

MOTOR behaviors can be significantly improved for collaborative tasks via interaction forces in physically interacting humans [1], [2]. Recently, the studies of physical interactions in human-robot systems have attracted growing research attention, such as applications in surgical robots [3] or the neuro-rehabilitation robots [4]. It is plausible that physical human-robot interaction (pHRI) is crucial to the success of collaborative robot behaviors [5], especially for wearable robotic exoskeletons.

When collaborative robots are in physical contact with humans to perform tasks, it is observed that robots that understand the movement intentions of operators can improve interaction and performance. A great deal of efforts have been devoted to revealing these outcoming [6], and motion intention of the user during physical interaction tasks can be estimated by force feedback [7], [32], hybrid perception [8], [9] or physiological signal recognition (like surface electromyogram) [10]–[12]. Thereby, the user's motion intention is prescribed as a reference trajectory or feedback enhancement of a robot. However, these approaches rely on accurate or computational modeling and trajectory generation with multi-parameter complex operations, or finite discrete motion signals obtained by online or offline training and demonstrations, leading to various restrictions in physically real interaction. In [13]–[16], the motion intention is defined as a set of states, e.g., the user's limb future position or motor primitives, which is capable of offering continuous movement prediction of the user's behavior. However, the parameters based on motion model in these methods are required to be either known or can be accurately estimated. Learning from but different from the aforementioned results and inspired by [17], this letter proposes an assimilation method to incorporate human motion intention by developing a virtual target, rather than direct estimation of the user's intention, to enable continuous prediction of future movement.

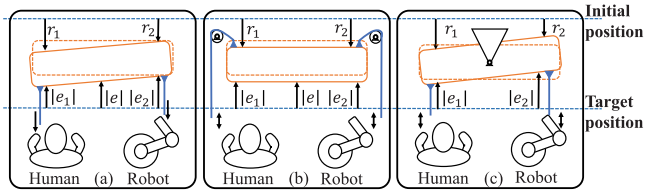

Fig. 1. Several different types of task models during pHRI. (a) The divisible task. (b) The interactive task. (c) The antagonistic tasks. e_i is the error relative to the target, and r_i is the reward added when the state is close to the target ($i = 1$ represents the human, and $i = 2$ represents the exoskeleton).

Once the user's motion intention could be estimated, interactive robots would be instructed to cooperate with human movement or counteract it. As shown in Fig. 1, a simple task where both interacting parties can pull a rope to approach the pallet is considered, which shows that different interaction modes bring differentiated results [18]. The orange dashed rectangular box represents the initial position of the pallet, while the orange solid box is the target position to be approached. In the divisible task, each operator contributes to its own subtask, where the two are independent (If $|e_1|\downarrow$ or $|e_2|\downarrow$, then $|e|\downarrow$). In the interactive task, two operators must cooperate to complete the task successfully

Manuscript received September 24, 2021; accepted January 11, 2022. Date of publication January 21, 2022; date of current version February 3, 2022. This letter was recommended for publication by Associate Editor C. Yang and Editor J. Kober upon evaluation of the reviewers' comments. This work was supported in part by the National Natural Science Foundation of China under Grant U1913601, the National Key Research and Development Program of China under Grants 2021YFF0501600 and 2018YFC2001602, and in part by the Major Science and Technology Projects of Anhui Province under Grant 202103a05020004. *(Corresponding author: Zhijun Li.)*

The authors are with the Department of Automation, University of Science and Technology of China, Hefei 230026, China, and also with the Institute of Artificial Intelligence, Hefei Comprehensive National Science Center, Hefei 230031, China (e-mail: lgxin16@mail.ustc.edu.cn; zjli@ieee.org; zkan@ustc.edu.cn).

This letter has supplementary downloadable material available at https://doi.org/10.1109/LRA.2022.3144537, provided by the authors.

Digital Object Identifier 10.1109/LRA.2022.3144537

(If $|e_1| \downarrow$ and $|e_2| \downarrow$, then $|e| \downarrow$). In the antagonistic tasks, the performance of one operator is against the other (If $|e_1| \downarrow$, then $|e_2| \uparrow$). Extensive efforts have been devoted in the last decades. Master-slave(or leader-follower) behaviour mode is widely used in human-robot systems, where the slave robot is fully controlled to follow the movement or force imposed by an operator [19]. This kind of control law fails to make the robot proactively adapt to movement during the interaction with the user. In [20], an adaptive motion generation strategy that employs a class of parameterized dynamical systems is designed to enable robots to compliantly follow the intention of human in a multi-task setting. In [21], an adaptive control strategy using the dynamical movement primitives is designed to estimate the human motor fatigue, which yields a sharp reduction in human efforts. Additionally, by fully utilizing the information offered by their interactions, more efficient task-sharing could be mutually beneficial for both the robot and its user [22]. In [23], [24], the robot adapts its control to the partner's behavior by shared control. In [25], a shared control architecture is used to appropriately fuse the human and the robot inputs to facilitate the human to freely navigate while avoiding obstacles. Game theory (GT) is also adopted to dissect diverse interactive behaviours. However, the knowledge of the partners dynamics and control strategies are often assumed in GT based framework, which are not always available in practice [26]. Other control methods are determined by interaction tasks, such as "less-than-needed assistance" to facilitate efforts in physical rehabilitation [27], or a "antagonistic behavior" that violates the operator's assumptions [28]. For instance, the surgical robot may need to suppress the surgeon's movements to avoid cutting important organs that the surgeon ignores [29]. However, these efforts focus on a single interactive behavior. To make it possible in completing more interaction, such as in Fig. 1, in this study, an assimilation control method is developed that allows smooth transitions of robot behavior from assistance to competition to facilitate human-robot interaction, without the need of manual guidance.

The robot's trajectory reconstruction during the pHRI in this study depends on the user's virtual target via force feedback. The impedance control is first proposed to address the instability caused by force control in [30]. Moreover, robot dynamics and interactive dynamics are required. In [31], [32], the movement of the robot is generated by the admittance control. Although the control purpose is to ensure tracking performance, the interaction force is treated as an external disturbance item, where the flexibility of the tracking is not considered. In [33], [34], reference trajectory adaptation is designed for the collaborative task, where human motion characteristics are considered. This letter designs a dynamic method by introducing the user's control gain to continuously predict the trajectory and develops an adaptive controller to track it.

There are three main differences in the proposed trajectory reconstruction assimilation control compared with other interaction control. First, a virtual target determined by human motion intention is designed in the assimilation control, which does not require accurate estimation of human control and eliminates many constraints in most existing methods, such as the knowledge of limb model or motion parameters [13]–[16], or sensing measurement [35]. Second, the assimilation control provides diverse interactive behaviors from assistance to competition determined by open parameters over the methods concerning roles switching [22]–[24]. Third, an adaptive controller is designed to enable the robot to track the reshaping trajectory accurately by utilizing the human virtual target while avoiding obstacles.

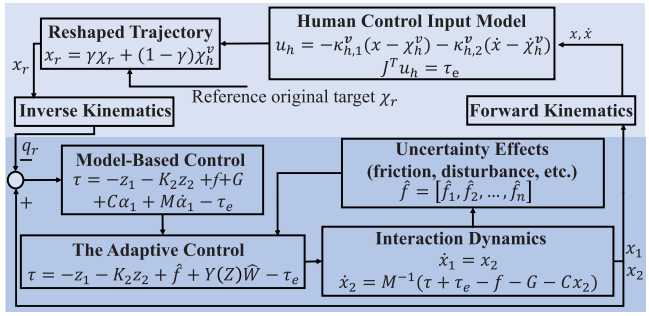

Fig. 2. The framework of the proposed assimilation control in pHRI.

Previous works that consider physical human-computer interaction include [32], [34], [36]–[40]. In [36], [37], coordination control is realized by the human-robot skill transfer utilizing the impedance parameters and interaction force. In [38], [39], human motion intention is obtained by interaction force to complete cooperative task. In [40], interpersonal collaboration models are considered to complete asymmetric cooperation control of dual-arm exoskeletons, which enables the robot to successfully track target with two operator. However, the above works only focus on the single mode of human-robot cooperative behavior.

In this letter, an assimilation control method for reshaping the trajectory according to the interactive environment during pHRI is proposed. First, a virtual target determined by human motion intention is designed to generate reference trajectory, without relying on accurate estimation of human control. The assimilation control then provides continuously changed interactive behaviors from assistance to competition determined by open parameters while avoiding obstacles. Finally, an adaptive controller is designed to enable the robot to track the generated trajectory accurately. The control strategy consists of two closed-loop, as shown in Fig. 2. The inner loop includes an adaptive controller that deals with unknown mass and moment of inertia in the robot's dynamics, while the outer loop takes the user's intention into account and adjusts the interaction model. The experiments performed on the exoskeleton demonstrate how the assimilation control method assists the subjects in movement or competes against them to produce antagonistic behavior for safe obstacle avoidance.

II. Preliminaries

A. Human-Robot System Dynamics

Consider an interactive task between a robotic exoskeleton with n degree of freedom (DOF) and a subject, where the dynamics of the robotic exoskeleton is

$$M(q)\ddot{q} + C(q,\dot{q})\dot{q} + G(q) + f = \tau + \tau_e(t) \tag{1}$$

where $q \in R^n$ is the joint position of the robotic exoskeleton, $\tau \in R^n$ is the control input to the exoskeleton's joint, $\tau_e \in R^n$ is the torque exerted by the user during the interaction between the exoskeleton and the human. $M(q) \in R^{n\times n}$, $C(q,\dot{q}) \in R^{n\times n}$, and $G(q) \in R^n$ are the inertia term, the centripetal and Coriolis term, and the gravitational term of the robotic exoskeleton, respectively, $f \in R^n$ represents the unknown uncertainties to the system, e.g., the friction coefficients, residual time-varying disturbances, such as stiction or torque ripple.

Property 1: [41] $\dot{M}(q) - 2C(q,\dot{q})$ is skew-symmetric, thus $\beta^T(\dot{M}(q) - 2C(q,\dot{q}))\beta = 0, \forall \beta \in R^n$.

Property 2: [42] $M^{-1}(q)$ exists, and is also positive definite and bounded, i.e., $\|M^{-1}(q)\| < \varpi$, where ϖ is a positive constant.

Property 3: [43] There exists a constant parameter $W \in R^m$ whose entries are determined by the robot's dynamics parameters including masses, moments of inertia, etc, such that the dynamic terms in Eq. (1) can be linearly parameterized as

$$M(q)\dot{\xi} + C(q,\dot{q})\xi + G(q) = Y(q,\dot{q},\xi,\dot{\xi})W \tag{2}$$

where $Y(q,\dot{q},\xi,\dot{\xi}) \in R^{n\times m}$ is the dynamic regressor matrix, and $\xi \in R^n$ is a vector of differentiable function.

Assumption 1: [44] The system's uncertainties representing the friction and disturbances f satisfy

$$\|f\| \le d_1 + d_2\|z_1\| + d_3\|\dot{z}_1\| \tag{3}$$

where d_1, d_2, and d_3 are positive constant, z_1 and $\dot{z}_1$ are the tracking error of the system and its derivative, respectiviely.

The dynamics in (1) can be rewritten in the task space as

$$M_x\ddot{x} + C_x\dot{x} + G_x + F_f = u + u_h \tag{4}$$

where $x \in R^m$ is the position of the exoskeleton' end effector, which can be computed based on forward kinematics as

$$x = \Phi(q) \tag{5}$$

$$\dot{x} = J(q)\dot{q} \tag{6}$$

where $\Phi(\bullet) \in R^n \to R^m$ is a nonlinear kinematic equation that maps the joint space to the task space and $J(q) \in R^{m\times n}$ is the Jacobian matrix of the exoskeleton. $u \in R^m$ denotes the input of the exoskeleton to the end effector, $u = J^{\dagger T}(q)\tau$, where $J^{\dagger T}(q)$ represents the pseudo inverse of $J^T(q)$, $u_h \in R^m$ denotes the interactive force which is exerted on the end effector by the human, $u_h = J^{\dagger T}(q)\tau_e$, and $F_f = J^{\dagger T}(q)f$. M_x, C_x, and G_x are all functions of q or $\dot{q}$ and the arguments of M_x, C_x and G_x are omitted for convenience of analysis. And $M_x = J^{\dagger T}(q)M(q)J^{\dagger}(q)$, $C_x = J^{\dagger T}(q)[C(q,\dot{q}) - M(q)J^{\dagger}(q)\dot{J}(q)]J^{\dagger}(q)$, $G_x = J^{\dagger T}(q)G(q)$.

Let $x_1 = [q_1, q_2, \ldots, q_n]^T$, $x_2 = [\dot{q}_1, \dot{q}_2, \ldots, \dot{q}_n]^T$, then the interaction dynamics can be written as:

$$\dot{x}_1 = x_2 \tag{7}$$

$$\dot{x}_2 = M(q)^{-1}(\tau + \tau_e - f - G(q) - C(q,\dot{q})x_2) \tag{8}$$

The purpose of the control is to ensure that the variable x_1 continuously tracks the desired trajectory of the joints, thus enabling the robot's end to track the target trajectory in the presence of an interaction force. Besides, the closed-loop signals need to be bounded and converged, which satisfies $|x_{1,i}(t)| < k_{ci}, i = 1, 2, \ldots, n, \forall t > 0$.

B. Assimilation of the Human's Intention

To efficiently adjust interaction behaviours, the robotic exoskeleton is required to know the human's target position. Supposing that q and $\dot{q}$ are available, x and $\dot{x}$ could be calculated. Then a control law τ could be generated to control the joints of the exoskeleton to perform the desired motion, which ensures the end position x moves to the target. In [2], a dynamics model is developed based on the interaction force that couples the participants' positions for physically interacting tasks. Assuming that the control input from the human is related to his own control gain, similar to [17], the force exerted to the exoskeleton by the human operator is modeled as

$$u_h = -\kappa_{h,1}(x - \chi_h) - \kappa_{h,2}(\dot{x} - \dot{\chi}_h) \tag{9}$$

where $\kappa_{h,1} \in R^{m\times m}$ and $\kappa_{h,2} \in R^{m\times m}$ are control gains, $\chi_h \in R^m$ is the human's target position. This model shows how the human operator interacts with the exoskeleton to move to the target position via control feedback, which will be exploited to generate the estimation of the human's target and then used in the control of the exoskeleton via u_h if $\kappa_{h,1}$ and $\kappa_{h,2}$ are known.

The human's control input u_h can be measured by a force sensor and the exoskeleton's position x and $\dot{x}$ can be obtained by (5) and (6) using q and $\dot{q}$. To eliminate the requirement that the control gains are estimated from the neuromechanics [45], the virtual human's target χ_h^ν is used, which is derived from randomly selected control gains through [17]

$$u_h = -\kappa_{h,1}^\nu(x - \chi_h^\nu) - \kappa_{h,2}^\nu(\dot{x} - \dot{\chi}_h^\nu) \tag{10}$$

where the virtual human control gains $\kappa_{h,1}^\nu, \kappa_{h,2}^\nu$ are predefined. For example, the average values measured from many people may be chosen as the virtual human control gains.

Eq. (9) indicates that the actual position x depends on the human's target position χ_h in the presence of interaction force u_h. In other words, the interaction is determined by the exoskeleton's position x and the human's target position χ_h. For example, it is considered to be the assistance when $x = \chi_h$, where the robot uses the human's target with no or less interaction force. When $x = \chi_r$ (χ_r is defined as the robot's original target position), the robot performs its original target χ_r independently. Moreover, $x = 2\chi_r - \chi_h$ may be viewed as antagonistic interaction and the robot follows its own target to restrain the human's target. These special cases reflect how the robot's interaction behaviors change by relying on the influence of the assimilation of the human's intention. Thus, skillfully planning the relationship between x and χ_h can realize specified and diverse behavior strategies during the interaction tasks.

By solving the differential equation (10), the virtual human's target is calculated as

$$\chi_h^\nu = \mathscr{C}_1 e^{c_1 t} + \mathscr{C}_2 \tag{11}$$

where $c_1 = -\frac{\kappa_{h,1}^\nu}{\kappa_{h,2}^\nu}$, $\mathscr{C}_1 = x - \dot{x}\frac{1}{c_1} + \frac{u_h}{\kappa_{h,1}^\nu}$, and $\mathscr{C}_2 = -\mathscr{C}_1$.

In order to generate a general interaction behaviour, a reshaped target x_r of the robot is designed according to the virtual

human's target by [17]

$$x_r = \gamma\chi_r + (1-\gamma)\chi_h^{\nu} \tag{12}$$

where the weight $\gamma \geq 0$ determines whether the exoskeleton performs cooperative or antagonistic behavior. Particularly, $\gamma = 0$ indicates assistive behaviour in which the exoskeleton mirrors the operator's control inputs. The exoskeleton is cooperative if $0 < \gamma < 1$. When $\gamma = 1$, the exoskeleton operates according to its own reference target χ_r while ignoring the interaction force from the operator. Finally, $\gamma > 1$ indicates antagonistic behaviour. Different tasks can have different values γ, which is task-dependent.

C. Control Design and Stability Analysis

Define the errors z_1 and z_2 as:

$$z_1 = x_1 - q_r \tag{13}$$

$$z_2 = x_2 - \alpha_1 \tag{14}$$

where q_r denotes the desired trajectory of the joints, $q_r = [q_{1r}, q_{2r}, \ldots, q_{nr}]^T$, $\alpha_1 \in R^n$ is the virtual control to z_1. And we have

$$\dot{z}_1 = \dot{x}_1 - \dot{q}_r = z_2 + \alpha_1 - \dot{q}_r \tag{15}$$

Consider $V_1 = \frac{1}{2} z_1^T z_1$ as a Lyapunov function candidate, and taking time derivative of V_1 yields

$$\dot{V}_1 = z_1^T \dot{z}_1 = z_1^T (z_2 + \alpha_1 - \dot{q}_r) \tag{16}$$

Let $\alpha_1 = \dot{q}_r - K_1 z_1$ with $K_1 \in R^{n\times n}$ and $\lambda_{min}(K_1) > 0$, and substitute it to (16):

$$\dot{V}_1 = -z_1^T K_1 z_1 + z_1^T z_2 \tag{17}$$

Differentiating (14) yields

$$\begin{aligned}\dot{z}_2 &= \dot{x}_2 - \dot{\alpha}_1 \\ &= M(q)^{-1}(\tau + \tau_e - f - G(q) - C(q,\dot{q})x_2) - \dot{\alpha}_1\end{aligned} \tag{18}$$

where $\dot{\alpha}_1 = -K_1\dot{z}_1 + \ddot{q}_r$. An augmented Lyapunov function is considered as $V_2 = V_1 + \frac{1}{2} z_2^T M(q) z_2$, so

$$\begin{aligned}\dot{V}_2 &= \dot{V}_1 + z_2^T M(q)\dot{z}_2 + \frac{1}{2} z_2^T \dot{M}(q) z_2 \\ &= -z_1^T K_1 z_1 + z_1^T z_2 + z_2^T(\tau + \tau_e - f - G(q) \\ &\quad - C(q,\dot{q})x_2 - M(q)\dot{\alpha}_1 + \frac{1}{2}\dot{M}(q) z_2)\end{aligned} \tag{19}$$

According (14) and Property 1, we have

$$\begin{aligned}\dot{V}_2 &= -z_1^T K_1 z_1 + z_1^T z_2 + z_2^T(\tau + \tau_e - f - G(q) \\ &\quad - C(q,\dot{q})(z_2 + \alpha_1) - M(q)\dot{\alpha}_1 + \frac{1}{2}\dot{M}(q) z_2) \\ &= -z_1^T K_1 z_1 + z_1^T z_2 + z_2^T(\tau + \tau_e - f \\ &\quad - G(q) - C(q,\dot{q})\alpha_1 - M(q)\dot{\alpha}_1)\end{aligned} \tag{20}$$

Thus, the control input could be designed as follows:

$$\tau = -z_1 - K_2 z_2 + f + G(q) + C(q,\dot{q})\alpha_1 + M(q)\dot{\alpha}_1 - \tau_e \tag{21}$$

where $K_2 \in R^{n\times n}$ and $\lambda_{min}(K_2) > 0$. However, the above control is not applicable due to the unavailable uncertainties f, and unknown dynamics terms of $G(q), C(q,\dot{q}), M(q)$. To address unknown dynamics, Property 3 is used and we have

$$Y(Z)W = G(q) + C(q,\dot{q})\alpha_1 + M(q)\dot{\alpha}_1 \tag{22}$$

where $Y(Z) \in R^{n\times m}$ is the dynamic regressor matrix, $Z = [x_1^T, x_2^T, \alpha_1^T, \dot{\alpha}_1^T]^T$, and $W \in R^m$ is a constant vector determined by the unknown dynamic parameters. Since uncertain robot's dynamics exists, such that

$$Y(Z)\hat{W} = \hat{G}(q) + \hat{C}(q,\dot{q})\alpha_1 + \hat{M}(q)\dot{\alpha}_1 \tag{23}$$

where $\hat{W}$ represents the estimate of W, and $\hat{G}(q)$, $\hat{C}(q,\dot{q})$, $\hat{M}(q)$ represent the approximate term for $G(q), C(q,\dot{q}), M(q)$, respectively, and $\hat{W}$ follows the updated law as

$$\dot{\hat{W}} = -\Gamma Y^T(Z) z_2 \tag{24}$$

where $\Gamma \in R^{m\times m}$ is a positive-definite symmetric matrix, which determines the rate of the updated. Therefore, instead of (21), an adaptive control law is written as

$$\tau = -z_1 - K_2 z_2 + \hat{f} + Y(Z)\hat{W} - \tau_e \tag{25}$$

where $\hat{f}$ (referred to Assumption (1)) is used to deal with the uncertainty effects (friction, disturbance, etc.) with

$$\hat{f} = [\hat{f}_1, \hat{f}_2, \ldots, \hat{f}_n]^T \tag{26}$$

$$\hat{f}_i = -(d_1 + d_2\|z_1\| + d_3\|\dot{z}_1\|)sgn(z_{2i}) \tag{27}$$

Theorem 1: Given the robotic dynamics (7) and (8), using (25), together with (26), and (27), and the updated law (24), the control signals z_1, z_2, $\tilde{W}$ converges asymptotically to zero in the closed-loop system.

Proof: Substituting the control (25) into (20)

$$\dot{V}_2 = -z_1^T K_1 z_1 - z_2^T K_2 z_2 + z_2^T(\hat{f} - f) + z_2^T Y(Z)\tilde{W} \tag{28}$$

where $\tilde{W} = \hat{W} - W$. The extended Lyapunov candidate is designed as

$$V_3 = V_2 + 1/2\tilde{W}^T\Gamma_i^{-1}\tilde{W} \tag{29}$$

Taking time derivative of V_3, we have

$$\begin{aligned}\dot{V}_3 &= \dot{V}_2 + \tilde{W}^T\Gamma_i^{-1}\dot{\tilde{W}} \\ &= -z_1^T K_1 z_1 - z_2^T K_2 z_2 + z_2^T(\hat{f} - f) \\ &\quad + z_2^T Y(Z)\tilde{W} + \tilde{W}^T\Gamma_i^{-1}\dot{\tilde{W}}\end{aligned} \tag{30}$$

Given $z_2^T Y(Z)\tilde{W} = \tilde{W}^T Y^T(Z) z_2$, $\dot{\tilde{W}} = \dot{\hat{W}}$ with (24), such that

$$\begin{aligned}z_2^T Y(Z)\tilde{W} + \tilde{W}^T\Gamma_i^{-1}\dot{\tilde{W}} &= \tilde{W}^T Y^T(Z) z_2 + \tilde{W}^T\Gamma_i^{-1}\dot{\tilde{W}} \\ &= \tilde{W}^T(Y^T(Z) z_2 + \Gamma_i^{-1}\dot{\tilde{W}}) = 0\end{aligned} \tag{31}$$

Since

$$z_2^T \hat{f} = \sum_{i=1}^{n} z_{2i}[-(d_1 + d_2\|z_1\| + d_3\|\dot{z}_1\|)sgn(z_{2i})]$$
$$= \sum_{i=1}^{n}[-(d_1 + d_2\|z_1\| + d_3\|\dot{z}_1\|)|z_{2i}|]$$
$$\leq \sum_{i=1}^{n}(-\|f\| \cdot |z_{2i}|) \quad (32)$$

$$-z_2^T f \leq \|z_2^T\| \cdot \|f\| \quad (33)$$

where $\|z_2^T\| = \sum_{i=1}^{n} |z_{2i}|$, such that

$$z_2^T(\hat{f} - f) \leq \sum_{i=1}^{n}(-\|f\| \cdot |z_{2i}|) + \|z_2^T\| \cdot \|f\| = 0 \quad (34)$$

Substituting (31) and (34) into (30), it can be derived that

$$\dot{V}_3 \leq -z_1^T K_1 z_1 - z_2^T K_2 z_2 \leq 0 \quad (35)$$

Thus the theorem is proved, and the controller is globally asymptotically stable. ■

Remark 1: As can be seen from the control law (22), (23) and (24), the controller uses only general information about the robot dynamic equation. The matrix $M(q)$, $C(q, \dot{q})$, and $G(q)$ are completely unknown and no information on their possible sizes is required. By utilizing the selected parameters, i.e., $K_1 = K_1^T > 0$ and $K_2 = K_2^T > 0$, linearized dynamics terms (22), and compensation terms (26) and (27) with respect to these uncertainties whose supremum is known, the adaptive control law (25) can ensure system's robustness and stability, even if the parameters are uncertain.

III. Experiments

A. Experimental Protocol

Experiments including two trials are carried out on the developed dual-arm exoskeleton robot to verify that whether the proposed trajectory assimilation control method can assist or resist the subject during the interactive task. Each side of the exoskeleton has six DOF actuated by the motor (Maxon motor. EC90/50/15flat, ELMO motion control LTD Driver), as shown in Fig. 3. A 6-axis force sensor (SRI. M3703 C) is equipped on the handle to measure the force, and the sampling frequency is set as 1000 Hz. The joint angular positions q of the exoskeleton can be measured by encoder (Netzer. DS25).

As shown in Fig. 4(a) and 5(a), the flexion/extension of the shoulder and elbow joint in one side of the exoskeleton is involved with the trials in X-Y plane, with the lengths of two links being $L_1 = 0.26\,m$ and $L_2 = 0.41\,m$ and the joint angles q_1 and q_2. Therefore, the dynamics of a 2-DOF robot is considered in this study. The regressor matrix $Y(Z)$ defined in (22) is constructed as

$$Y(Z) = \begin{bmatrix} Y_{11} & Y_{12} & Y_{13} & Y_{14} & Y_{15} \\ Y_{21} & Y_{22} & Y_{23} & Y_{24} & Y_{25} \end{bmatrix} \quad (36)$$

where $\alpha_1 = [\alpha_{11}, \alpha_{12}]^T$, $\dot{\alpha}_1 = [\dot{\alpha}_{11}, \dot{\alpha}_{12}]^T$, $Y_{11} = \dot{\alpha}_{11}$, $Y_{12} = \dot{\alpha}_{11} + \dot{\alpha}_{12}$, $Y_{13} = (2\dot{\alpha}_{11} + \dot{\alpha}_{12})\cos(q_2) - \alpha_{12}(\dot{q}_1 + \dot{q}_2) - \alpha_{11}\dot{q}_2\sin(q_2)$, $Y_{14} = \cos(q_1)$, $Y_{15} = \cos(q_1 + q_2)$, $Y_{21} = 0$, $Y_{22} = \dot{\alpha}_{11} + \dot{\alpha}_{12}$, $Y_{23} = \dot{\alpha}_{11}\cos(q_2) + \alpha_{11}\dot{q}_1\sin(q_2)$, $Y_{24} = 0$, $Y_{25} = \cos(q_1 + q_2)$. The constant vector W is specified as $W = [W_1, W_2, W_3, W_4, W_5]^T$, $W_1 = m_1 L_{c1}^2 + m_2 L_1^2 + I_{c1}$, $W_2 = m_2 L_{c2}^2 + I_{c2}$, $W_3 = m_2 L_1 L_{c2}$, $W_4 = m_1 g L_{c1} + m_2 g L_1$, $W_5 = m_2 g L_{c2}$, where m_1 and m_2 are the unknown masses of the links, L_{c1} and L_{c2} are the unknown length from the centroid of the joint to the center of gravity, I_{c1} and I_{c2} are the unknown inertias of the links around the center of gravity, and g is the acceleration of gravity.

Fig. 3. Experimental platform where the subject with a robotic exoskeleton performs the motion with the robot.

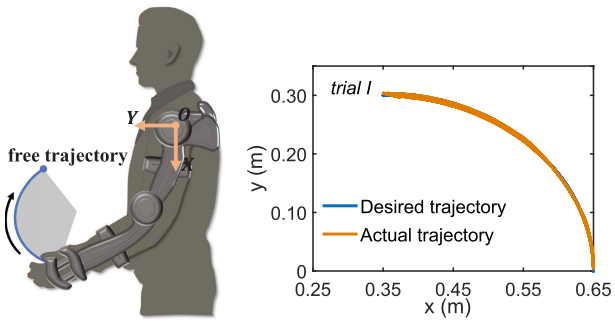

Fig. 4. Experimental results of the trial I of a representative participant, where the exoskeleton drives the subject to track a free trajectory, and the weight γ is 1. (a) Schematic of tracking a free trajectory. (b) The tracking performance of the robot's end in the task space.

Initially, all subjects are required to wear the exoskeleton to track the same preset desired trajectory $x = [X, Y]^T$, which satisfies the function with respect to time t as

$$\begin{cases} X = 0.35 + 0.3cos\left(-\frac{\pi}{4}cos\left(\frac{\pi}{8}t\right) + \frac{\pi}{4}\right) & (37) \\ Y = 0.3sin\left(-\frac{\pi}{4}cos\left(\frac{\pi}{8}t\right) + \frac{\pi}{4}\right) & (38) \end{cases}$$

It can be seen that the trajectory is a quarter arc with a radius of $0.3\,m$ around (0.35,0) of the center. The velocity of the end is time-varying and satisfies a sinusoidal function with a period of 16 seconds.

In the trial I, the robot drives the subject to follow a free trajectory as shown in Fig. 4(a), where there are no obstacles and

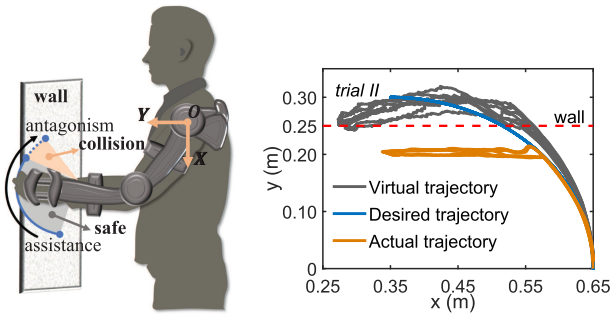

(a) (b)

Fig. 5. Experimental results of the trial II, where the robotic exoskeleton adjusts the target trajectory using dynamic γ while interacting with the subject from assisting to antagonism. The virtual wall is invisible in front of the subject. (a) Schematic of the tracing task with an invisible wall. (b) Variation of trajectory value of the end position in the task space, which includes the virtual human's target (the gray solid line), the original desired or reference target (the blue solid line), and the reshaped target (the orange solid line).

TABLE I
PARAMETERS OF THE CONTROLLER

Parameters	Description	Value
$\kappa_{h,1}^{v}$	Control Gain	diag(8, 10)
$\kappa_{h,2}^{v}$	Control Gain	diag(0.9, 0.9)
K_1	Error Gain	diag(6.5, 25)
K_2	Error Gain	diag(1.5, 9.5)
Γ	Adaptation Parameter	$0.0001I_5$
$[d_1, d_2, d_3]$	Compensation Parameters	[1, 2, 4]

γ is 1. In the trial II, a virtual wall is set 0.25 m away from the subject and the exoskeleton along the Y-axis, and the exoskeleton needs to cooperate with the subject to perform a safe interactive task using dynamic γ, as shown in Fig. 5(a). During the trials, the subjects hold the handle and apply proper force according to the scene to generate a reshaped reference trajectory. The preset reference trajectory and the end position of the subject will be displayed on the computer screen in real-time during the interaction, so that the exoskeleton can adjust the interactive behavior depending on a reshaped reference trajectory. Three subjects are informed of the requirements in advance and participated in the experiments. Additionally, they are also provided the informed consent. Approval of all ethical and experimental procedures and protocols is granted by Ethics Committee of Yueyang Integrated Traditional Chinese and Western Medicine Hospital Affiliated to Shanghai University of Traditional Chinese Medicine (Approval No. 2019–014).

B. Experimental Results

Two trials demonstrate how to adjust the target trajectory x_r depending on the force exerted by the subject during the interaction. The control gains and related parameters are listed in Table I, where $I_5 \in R^{5\times5}$ is the identity matrix.

1) The Exoskeleton Drives the Subject: In the trial I, the subjects' shoulders and elbows are relaxed, and the exoskeleton drives the subject to perform a $\frac{1}{4}$ circle of the desired trajectory

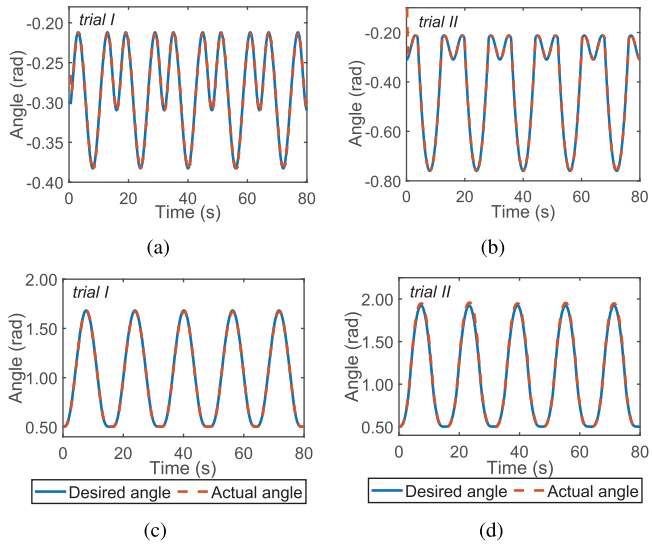

(a) (b) (c) (d)

Fig. 6. Experimental results of the trial I and II. (a) and (b) The tracking performance of the shoulder joint. (c) and (d) The tracking performance of the elbow joint.

and the weight is set as the constant $\gamma = 1$, which is shown in Fig. 4. During the interaction, the subjects' arm is relaxed, and the trajectory does not reshape. Fig. 4(b) shows the tracking trajectory of the actual position and the desired position of the robot in the task space, and Fig. 6(a) and 6(c) show the tracking performance of the shoulder and elbow joints' angles, respectively. The results indicate that the proposed control scheme can achieve stable assisted motion in this scenario and the designed adaptive control law can ensure robust tracking performance with the uncertainty effects of the system.

2) Dynamic Adjustment of Interactive Behavior: In the trial II, the virtual wall is invisible to the subject and is assumed to be known to the robot. The assimilation control could estimate the subject's target when approaching the wall, and foresee a collision, so that it can reshape the exoskeleton' reference trajectory by dynamically adjusting the value of γ using

$$\gamma = \begin{cases} 10p, & 0 \le p < 0.2 \\ 2, & 0.2 \le p \end{cases} \tag{39}$$

where p is defined as the distance between the subject and the invisible wall along Y axis. With γ increased, the continuous transition of the robot from assisting to antagonism is arising while there is a virtual obstacle. In full antagonism ($\gamma = 2$), the reshaped target trajectory is set to $x_r = x$ (the orange solid line), thus maintaining its current state.

Fig. 5 shows how the exoskeleton uses the proposed assimilation control to achieve a series of naturally changing interactive behaviors. At the initial moment, the trajectory reshaping controller parameter γ is 0. At this time, the exoskeleton robot follows the subject's movement, and the parameter γ gradually increases as the subject moves. When γ increases to 2, the reshaped reference trajectory of the exoskeleton robot remains unchanged in the Y direction, leaving the movement in the X direction. Therefore, the dynamic adjustment of γ makes the

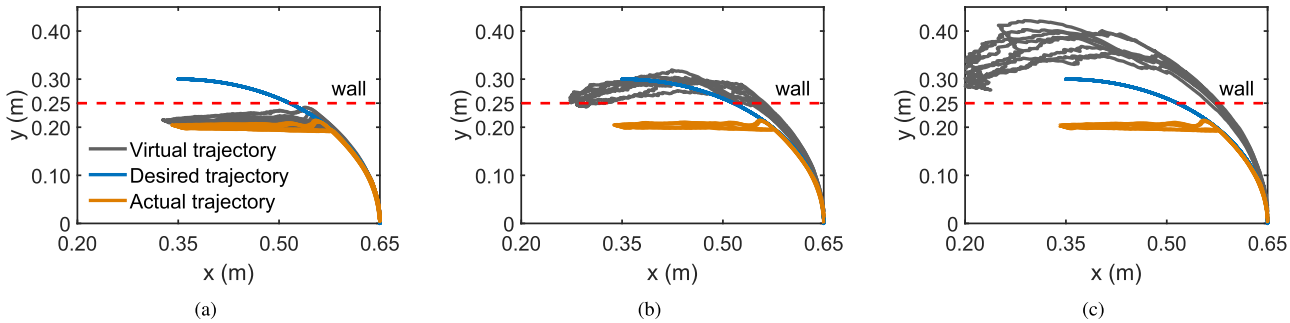

Fig. 7. The experiments demonstrate how the trajectory reshaping assimilation controller can simultaneously assist in free movement and prevent participants from colliding with obstacles under the different control gains. The sample experimental results of representative participant's interacting under (a) stiff control gain, (b) medium control gain and (c) compliant control gain.

TABLE II
THE PARAMETERS OF DIFFERENT CONTROL GAIN

Parameters	$\kappa_{h,1}^{\nu}$	$\kappa_{h,2}^{\nu}$
Stiff Control Gain	diag(15, 20)	diag(1.5, 1.5)
Medium Control Gain	diag(8, 10)	diag(0.9, 0.9)
Compliant Control Gain	diag(5, 6)	diag(0.4, 0.5)

interactive behavior between the exoskeleton and the human gradually changed from assistance to confrontation.

It is worth noting that after the parameter γ is increased to 2, the coordinate value of the Y direction of the target trajectory in the task space is nearly unchanged. At this time, the speed has a step jump, and the chattering occurring at (0.5736, 0.2) of the coordinate point in Fig. 5(b) indicates that the exoskeleton begins to compete against the subject, then converging to zero in error fast and tending to be stable in tracking synchronously. The experimental results show that the trajectory reshaping assimilation controller can effectively estimate the subject's motion intention, dynamically adjust the interactive behavior according to the interactive scene, and achieve obstacle avoidance through reshaped trajectory. Fig. 6(b) and 6(d) show the tracking performance of the shoulder and elbow joints' angles, respectively, which verifies that the controller can ensure the stability of tracking during dynamic interactive behaviors.

Further, we verify and test the effectiveness of the assimilation control methods under the three control gains: stiff control gain ($\kappa_{h,1}^{\nu}$= diag(15,20), $\kappa_{h,2}^{\nu}$= diag(1.5,1.5)), medium control gain ($\kappa_{h,1}^{\nu}$= diag(8,10), $\kappa_{h,2}^{\nu}$= diag(0.9,0.9)), and compliant control gain ($\kappa_{h,1}^{\nu}$= diag(5,6), $\kappa_{h,2}^{\nu}$= diag(0.4,0.5)) (Table II). Fig. 7 shows the sample experimental results of representative participant's interacting under stiff control gain, medium control gain and compliant control gain. When the human control gain is small, the derived virtual target is far from the reference trajectory. When the control gain is large, the derived virtual target is close and still larger than the reference trajectory. Interestingly, all trajectory reshaping assimilation controllers can prevent collisions effectively and provide safe interaction.

Depending on the humans virtual target, the proposed trajectory reconstruction assimilation control can determine the robot's behavior and provide motion guidance and safer obstacle avoidance from the assistance behavior to the antagonism. However, this method requires a priori or experimental human control gain. A near future prediction of avoiding collisions during three different control gains experiments has proved to be useful. However, how to identify the optimal value for the control gain and assistive or resisted time determined by the weight is critical to the application, such as physical rehabilitation and robot-assisted surgery.

IV. CONCLUSION

This letter introduces a trajectory reshaping assimilation control strategy to properly change the physical interaction behaviors between robots and humans. The control method allows the robot to estimate the human movement using the human's target position, so the human's near future behavior will be predicted. The stability and robustness of the controller are proved. The verified experiments show that the proposed method can assist human movement or resist human to avoid collisions, which shows a flexible and broader spectrum levels of interaction behaviors. Future work will focus on the effective determination of control gain through prior knowledge and reinforcement learning. Additionally, extensive experimental research should be conducted to find an acceptable level, where we can tell when assistance or confrontation behavior is acceptable during the practical application such as the operation.

REFERENCES

[1] G. Ganesh, A. Takagi, R. Osu, T. Yoshioka, M. Kawato, and E. Burdet, "Two is better than one: Physical interactions improve motor performance in humans," *Sci. Rep.*, vol. 4, pp. 1–7, Jan. 2014.
[2] A. Takagi, G. Ganesh, T. Yoshioka, M. Kawato, and E. Burdet, "Physically interacting individuals estimate the partners goal to enhance their movements," *Nature Hum. Behav.*, vol. 1, no. 3, pp. 1–6, Mar. 2017.
[3] H. Su, C. Yang, G. Ferrigno, and E. De Momi, "Improved human-robot collaborative control of redundant robot for teleoperated minimally invasive surgery," *IEEE Robot. Automat. Lett.*, vol. 4, no. 2, pp. 1447–1453, Apr. 2019.
[4] H. Yu, S. Huang, G. Chen, Y. Pan, and Z. Guo, "Human-robot interaction control of rehabilitation robots with series elastic actuators," *IEEE Trans. Robot.*, vol. 31, no. 5, pp. 1089–1100, Oct. 2015.
[5] Y. Liu, Z. Li, H. Liu, and Z. Kan, "Skill transfer learning for autonomous robots and human-robot cooperation: A survey," *Robot. Auto. Syst.*, vol. 128, pp. 1–11, Jun. 2020.

[6] D. P. Losey, C. G. McDonald, E. Battaglia, and M. K. OMalley, "A review of intent detection, arbitration, and communication aspects of shared control for physical human-robot interaction," *Appl. Mechanics Rev.*, vol. 70, no. 1, Feb. 2018.

[7] H. Li *et al.*, "Stable and compliant motion of physical human-robot interaction coupled with a moving environment using variable admittance and adaptive control," *IEEE Robot. Automat. Lett.*, vol. 3, no. 3, pp. 2493–2500, Jul. 2018.

[8] Y. Li, J. Eden, G. Carboni, and E. Burdet, "Improving tracking through human-robot sensory augmentation," *IEEE Robot. Automat. Lett.*, vol. 5, no. 3, pp. 4399–4406, Jul. 2020.

[9] X. Yu, W. He, Q. Li, Y. Li, and B. Li, "Human-robot co-carrying using visual and force sensing," *IEEE Trans. Ind. Electron.*, vol. 68, no. 9, pp. 8657–8666, Sep. 2021.

[10] R. Meattini, D. Chiaravalli, G. Palli, and C. Melchiorri, "sEMG-Based human-in-the-loop control of elbow assistive robots for physical tasks and muscle strength training," *IEEE Robot. Automat. Lett.*, vol. 5, no. 4, pp. 5795–5802, Oct. 2020.

[11] G. Li, Z. Li, J. Li, Y. Liu, and H. Qiao, "Muscle synergy-based planning and neural-adaptive control for a prosthetic arm," *IEEE Trans. Artif. Intell.*, vol. 2, no. 5, pp. 424–436, Oct. 2021.

[12] Y. Liu, Z. Li, H. Liu, Z. Kan, and B. Xu, "Bioinspired embodiment for intelligent sensing and dexterity in fine manipulation: A. survey," *IEEE Trans. Ind. Informat.*, vol. 16, no. 7, pp. 4308–4321, Jul. 2020.

[13] J. Lanini, H. Razavi, J. Urain, and A. Ijspeert, "Human intention detection as a multiclass classification problem: Application in physical human-robot interaction while walking," *IEEE Robot. Automat. Lett.*, vol. 3, no. 4, pp. 4171–4178, Oct. 2018.

[14] S. Javdani, H. Admoni, S. Pellegrinelli, S. S. Srinivasa, and J. A. Bagnell, "Shared autonomy via hindsight optimization for teleoperation and teaming," *Int. J. Robot. Res.*, vol. 37, no. 7, pp. 717–742, 2018.

[15] K. Alevizos, C. Bechlioulis, and K. Kyriakopoulos, "Physical human-robot cooperation based on robust motion intention estimation," *Robotica*, vol. 38, no. 10, pp. 1842–1866, Sep. 2020.

[16] J. R. Medina, T. Lorenz, and S. Hirche, "Synthesizing anticipatory haptic assistance considering human behavior uncertainty," *IEEE Trans. Robot.*, vol. 31, no. 1, pp. 180–190, Feb. 2015.

[17] A. Takagi, Y. Li, and E. Burdet, "Flexible assimilation of human's target for versatile human-robot physical interaction," *IEEE Trans. Haptics*, vol. 14, no. 2, pp. 421–431, Apr.-Jun. 2021.

[18] N. Jarrass, T. Charalambous, and E. Burdet, "A framework to describe, analyze and generate interactive motor behaviors," *PLoS One*, vol. 7, no. 11, pp. 1–13, Nov. 2012.

[19] J. Singh, A. R. Srinivasan, G. Neumann, and A. Kucukyilmaz, "Haptic-guided teleoperation of a 7-DoF collaborative robot arm with an identical twin master," *IEEE Trans. Haptics*, vol. 13, no. 1, pp. 246–252, Jan.-Mar. 2020.

[20] M. Khoramshahi and A. Billard, "A dynamical system approach to task adaptation in physical human-robot interaction," *Auton. Robots*, vol. 43, no. 4, pp. 927–946, 2019.

[21] L. Peternel *et al.*, "Robot adaptation to human physical fatigue in human-robot co-manipulation," *Auton. Robots*, vol. 42, pp. 1011–1021, 2018.

[22] N. Amirshirzad, A. Kumru, and E. Oztop, "Human adaptation to human-robot shared control," *IEEE Trans. Human-Mach. Syst.*, vol. 49, no. 2, pp. 126–136, Apr. 2019.

[23] Y. Li, K. P. Tee, R. Yan, W. L. Chan, and Y. Wu, "A framework of human-robot coordination based on game theory and policy iteration," *IEEE Trans. Robot.*, vol. 32, no. 6, pp. 1408–1418, Dec. 2016.

[24] Y. Li, G. Carboni, F. Gonzalez, D. Campolo, and E. Burdet, "Differential game theory for versatile physical human-robot interaction," *Nature Mach. Intell.*, vol. 1, pp. 36–43, Jan. 2019.

[25] C. Ton, Z. Kan, and S. S. Mehta, "Obstacle avoidance control of a human-in-the-loop mobile robot system using harmonic potential fields," *Robotica*, vol. 36, no 4, pp. 463–483. 2018.

[26] C. Messeri, G. Masotti, A. M. Zanchettin, and P. Rocco, "Human-robot collaboration: Optimizing stress and productivity based on game theory," *IEEE Robot. Automat. Lett.*, vol. 6, no. 4, pp. 8061–8068, Oct. 2021.

[27] D. J. Reinkensmeyer *et al.*, "Computational neurorehabilitation: Modeling plasticity and learning to predict recoverys," *J. Neuroeng. Rehabil.*, vol. 13, no. 42, pp. 1–25, Apr. 2016.

[28] T. Nierhoff, K. Leibrandt, T. Lorenz, and S. Hirche, "Robotic billiards: Understanding humans in order to counter them," *IEEE Trans. Cybern.*, vol. 46, no. 8, pp. 1889–1899, Aug. 2016.

[29] F. Abdollahi *et al.*, "Error augmentation enhancing arm recovery in individuals with chronic stroke: A. randomized crossover design," *Neurorehabilitation Neural Repair*, vol. 28, pp. 120–128, Feb. 2014.

[30] N. Hogan, "Impedance control an approach to manipulation. I-theory. II-Implementation. III-Applications," *Trans. ASME J. Dyn. Syst., Meas., Control*, vol. 107, pp. 1–24, 1985.

[31] I. Ranatunga, F. L. Lewis, D. O. Popa, and S. M. Tousif, "Adaptive admittance control for human-robot interaction using model reference design and adaptive inverse filtering," *IEEE Trans. Control Syst. Technol.*, vol. 25, no. 1, pp. 278–285, Jan. 2017.

[32] Z. Li, B. Huang, Z. Ye, M. Deng, and C. Yang, "Physical human-robot interaction of a robotic exoskeleton by admittance control," *IEEE Trans. Ind. Electron.*, vol. 65, no. 12, pp. 9614–9624, Dec. 2018.

[33] L. Roveda, M. Magni, M. Cantoni, D. Piga, and G. Bucca, "Human-robot collaboration in sensorless assembly task learning enhanced by uncertainties adaptation via bayesian optimization," *Robot. Auton. Syst.*, vol. 136, 2021.

[34] X. Wu, Z. Li, Z. Kan, and H. Gao, "Reference trajectory reshaping optimization and control of robotic exoskeletons for human-robot co-manipulation," *IEEE Trans. Cybern.*, vol. 50, no. 8, pp. 3740–3751, Aug. 2020.

[35] M. Laghi *et al.*, "Shared-autonomy control for intuitive bimanual telemanipulation," in *Proc. IEEE-RAS 18th Int. Conf. Humanoid Robots (Humanoids)*, 2018, pp. 1–9.

[36] B. Huang, Z. Li, X. Wu, A. Ajoudani, A. Bicchi, and J. Liu, "Coordination control of a dual-arm exoskeleton robot using human impedance transfer skills," *IEEE Trans. Syst., Man, Cybern. Syst.*, vol. 49, no. 5, pp. 954–963, May. 2019.

[37] Z. Li, C. Xu, Q. Wei, C. Shi, and C. -Y. Su, "Human-inspired control of dual-arm exoskeleton robots with force and impedance adaptation," *IEEE Trans. Syst., Man, Cybern. Syst.*, vol. 50, no. 12, pp. 5296–5305, Dec. 2020.

[38] Z. Li, B. Huang, A. Ajoudani, C. Yang, C. Y. Su, and A. Bicchi, "Asymmetric bimanual control of dual-arm exoskeletons for human-cooperative manipulations," *IEEE Trans. Robot.*, vol. 34, no. 1, pp. 264–271, Feb. 2018.

[39] X. Wu and Z. Li, "Cooperative manipulation of wearable dual-arm exoskeletons using force communication between partners," *IEEE Trans. Ind. Electron.*, vol. 67, no. 8, pp. 6629–6638, Aug. 2020.

[40] Z. Li, G. Li, X. Wu, Z. Kan, H. Su, and Y. Liu, "Asymmetric cooperation control of dual-arm exoskeletons using human collaborative manipulation models," *IEEE Trans. Cybern.*, to be published, doi: 10.1109/TCYB.2021.3113709.

[41] J.-J. E. Slotine and W. Li, "On the adaptive control of robot manipulators," *Int. J. Robot. Res.*, vol. 6, no. 3, pp. 49–59, 1987.

[42] S. S. Ge, C. C. Hang, T. H. Lee, and T. Zhang, *Stable Adaptive Neural Network Control*. New York, USA: Springer Science & Business Media, 2013.

[43] S. Arimoto, *Control Theory of Non-Linear Mechanical Systems: A Passivity-Based and Circuit-Theoretic Approach*. London, U.K.: Oxford Univ. Press, 1996.

[44] C. -Y. Su and T. -P. Leung, "A sliding mode controller with bound estimation for robot manipulators," *IEEE Trans. Robot. Automat.*, vol. 9, no. 2, pp. 208–214, Apr. 1993.

[45] E. Burdet, D. W. Franklin, and T. E. Milner, *Human Robotics: Neuromechanics and Motor Control*. Cambridge, Massachusetts, London, U.K.: MIT Press, Sep. 2013.